analytical chemistry

Article

pubs.acs.org/ac

Minimizing Fouling at Hydrogenated Conical-Tip Carbon Electrodes during Dopamine Detection in Vivo

Shaneel Chandra,[§,∥] Anthony D. Miller,[†] Avi Bendavid,[‡] Philip J. Martin,[‡] and Danny K. Y. Wong*[,§]

Departments of [§]Chemistry and Biomolecular Sciences and [†]Psychology, Macquarie University, Sydney, New South Wales 2109, Australia

[‡]CSIRO Materials Science and Engineering, P.O. Box 218, Lindfield, New South Wales 2070, Australia

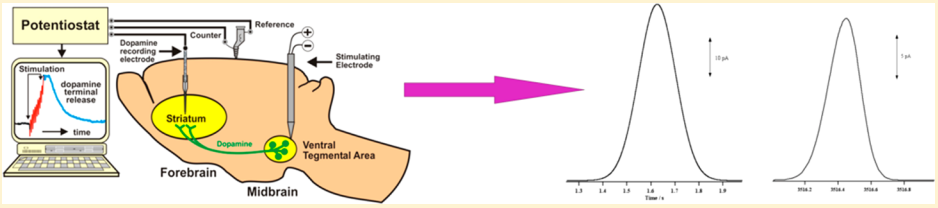

ABSTRACT: In this paper, physically small conical-tip carbon electrodes (~2−5 μm diameter and ~4 μm axial length) were hydrogenated to develop a probe capable of withstanding fouling during dopamine detection in vivo. Upon hydrogenation, the resultant hydrophobic sp^3 carbon surface deters adsorption of amphiphilic lipids, proteins, and peptides present in extracellular fluid and hence minimizes electrode fouling. These hydrogenated carbon electrodes showed a 35% decrease in sensitivity but little change in the limit of detection for dopamine over a 7-day incubation in a synthetic laboratory solution containing 1.0% (v/v) caproic acid (a lipid), 0.1% (w/v) bovine serum albumin and 0.01% (w/v) cytochrome C (both are proteins), and 0.002% (w/v) human fibrinopeptide B (a peptide). Subsequently, during dopamine detection in vivo, over 70% of the dopamine oxidation current remained after the first 30 min of a 60-min experiment, and at least 50% remained over the next half-period at the hydrogenated carbon electrodes. On the basis of these results, an initial average electrode surface fouling rate of 1.2% min^{-1} was estimated, which gradually declined to 0.7% min^{-1}. These results support minimal fouling at hydrogenated carbon electrodes applied to dopamine detection in vivo.

Dopamine is a major neurotransmitter involved in initiating many behavioral responses to various stimuli.[1] In addition, it also plays a crucial role in the functioning of the central nervous, cardiovascular, renal, and hormonal systems, as well as emotional and reward processes.[2] As dopamine can be easily oxidized, electrochemistry, in conjunction with anatomical, physiological, and pharmacological evidence, has been developed as a sensitive, real-time detection technique for dopamine. For example, using fast-scan cyclic voltammetry, Park et al.[3] were able to selectively and simultaneously monitor dopamine in the anterior nucleus accumbens and norepinephrine in the ventral bed nucleus of the stria terminalis in the brain of an anesthetised rat. Bledsoe et al.[4] developed a device called the Wireless Instantaneous Neurotransmitter Concentration System that incorporates fast-scan cyclic voltammetry to perform real-time, spatially and chemically resolved neurotransmitter measurements during functional neurosurgery. Also, Sombers et al.[5] have studied the effects of pharmacological or physicochemical parameters on the characteristics of dopamine amperometric peaks to gain further knowledge about exocytosis.

During electrochemical detection of dopamine in vivo, a carbon fiber electrode is often positioned in close proximity to a stimulated dopamine cell such that released dopamine rapidly diffuses toward the electrode to make physical contact for electron transfer. Such an electrode typically consists of an approximately 2.5−7 μm tip diameter carbon fiber sealed in a glass capillary with an ~100 μm length protruding the capillary.[6,7] Constant-potential amperometric detection at the electrode yields a peak-shaped signal in which the rising portion corresponds to the oxidation of dopamine that initiates contact with the electrode surface, while the declining portion arises from the waning concentration of dopamine around the electrode as it is subjected to uptake and diffusion processes.[8]

Our laboratory has developed structurally small conical-tip carbon electrodes by thermally pyrolyzing acetylene to form a carbon deposit at the tip and on the shank of a quartz capillary already pulled down to a tapered end.[9−11] Recent simulation work[12] indicates that these electrodes consist of a cone-shaped carbon deposit with a typical tip diameter of 2−5 μm and an axial length of 4 μm around the pulled capillary. Compared to carbon fiber electrodes, the glass substrates of conical-tip carbon electrodes are mechanically stronger and their sharp tips aid in easy membrane penetration during implantation in an in vivo experiment. Furthermore, the insulating plane at the finite fiber-capillary junction on carbon fiber electrodes limits mass transport of analyte to the base edge of the electrode, whereas the open-ended base edge on a conical-tip electrode is more accessible. Therefore, these conical-tip carbon electrodes of a similar

Received: October 11, 2013
Accepted: February 3, 2014

   dx.doi.org/10.1021/ac403283t | *Anal. Chem.* XXXX, XXX, XXX−XXX

dimension to carbon fiber electrodes display an improved signal-to-noise ratio in detecting dopamine in vivo.[11]

A problem often encountered in electrochemical detection of dopamine is electrode fouling caused by adsorption of amphiphilic high molecular weight proteins, lipids, and peptides present in extracellular fluid. This barrier prohibits dopamine from making contact with the electrode surface, resulting in a diminishing transient electrode response. Consequently, distorted voltammetric signals and suppressed electrode sensitivity are observed.[13,14] Considerable research effort has been devoted to addressing electrode fouling, for example, the incorporation of films such as the negatively charged Nafion,[15] which prevents electrode fouling as well as selectively allowing cationic dopamine (under physiological pH) to access the electrode surface. More recently, we have evaluated the effectiveness of *p*-phenylacetate film-coated conical-tip carbon electrodes in minimizing fouling.[16] The film was demonstrated to have aided in retarding the fouling rate at the electrodes by approximately a factor of 2 compared to bare conical-tip carbon electrodes. Similarly, fast scan cyclic voltammetry has also often been used to enable detection and quantification of dopamine before severe fouling took place.[17−19]

Alternatively, diamond film-immobilized electrodes, such as those consisting of small faceted crystals (100−200 nm in size) and doped with boron, have been developed as fouling-resistant electrochemical sensors.[17,20−22] As the closely adjoining, well-faceted microcrystallites on the diamond films are hydrogen-terminated, they give rise to a hydrophobic surface that is nonpolar and inert for adsorption of amphiphilic species. These electrodes were demonstrated to minimize fouling during in vivo dopamine detection.[21] Similar to diamond, hydrogenated graphitic carbon, which primarily consists of sp^3 carbon, has been demonstrated to yield hydrophobicity, making the carbon surface less susceptible to fouling by large amphiphilic molecules.[23,24] Our laboratory has previously reported some preliminary results in using hydrogenated carbon electrodes to resist fouling in vitro.[9] These electrodes were hydrogenated using a remote plasma hydrogenation process before being incubated in 0.1% bovine serum albumin for 3 weeks. Cyclic voltammetry of dopamine at these electrodes demonstrated a 5% decrease in limiting current, which compared favorably to a more severe 29% reduction at bare carbon electrodes.

In this paper, we present an alternative methodology involving radio frequency plasma for hydrogenation to fabricate physically small electrodes suitable for in vivo detection of dopamine. We have initially studied the electrochemistry of the hydrogenated conical-tip carbon electrodes, followed by an assessment of their fouling resistance in synthetic solutions in vitro and during detection of dopamine in anesthetised rat brain.

EXPERIMENTAL SECTION

Reagents and Materials. American Chemical Society analytical grade dopamine, citric acid, potassium chloride, potassium ferricyanide, sodium phosphate dibasic heptahydrate, hexanoic acid, human fibrinopeptide B, cytochrome C, bovine serum albumin, and graphite powder were purchased from Sigma Aldrich (Sydney, Australia). Ultra-high-purity acetylene and nitrogen gases were purchased from BOC Gases, Australia. Hexaminеruthenium(III) chloride was obtained from Stremm Chemicals (Newburyport, MA, USA). All chemicals and reagents were used without further purification. All solutions and supporting electrolytes were prepared daily using ultrapure (Milli-Q) water (18.2 MΩ cm at 25 °C) and were purged with nitrogen for 5 min preceding analysis. Urethane (dissolved in distilled water) was purchased from ICN Biochemicals (Seven Hills, NSW, Australia).

Instrumentation and Apparatus. Quartz capillaries (1 mm outside diameter, 0.5 mm inside diameter, and 75 mm length, Sutter Instrument Company, Novato, CA, USA) were pulled to a fine tapered end using a Model P-2000 Sutter Puller (Sutter Instrument Co.). Electrochemical measurements including cyclic voltammetry and fixed-potential amperometry were performed using a low-current potentiostat (eDAQ Pty Ltd., Sydney, NSW, Australia) operated using EChem version 2.1.2 software on a PC via an E-corder interface (eDAQ Pty Ltd.). A single-compartment, three-electrode glass cell that accommodates a Ag|AgCl reference electrode, a platinum wire counter electrode, and either a bare or a hydrogenated conical-tip carbon working electrode was used. All measurements at electrodes were conducted within 3 h of fabricating them at room temperature (25 °C). To isolate noise and interruptions from the mains, all experiments were performed in a Faraday cage positioned as far as possible from power leads, and mains-powered equipment.

Fabrication of Hydrogenated Conical-Tip Carbon Electrodes. Initially, physically small conical-tip carbon electrodes were fabricated as described previously.[10] Briefly, after pulling a quartz capillary down to a fine tip, it was housed in a larger nuclear magnetic resonance tube such that acetylene gas was delivered into the former at 50 kPa and a nitrogen stream was counter-flowing through the latter at 60 mL min^{-1}. The acetylene gas was thermally pyrolyzed to form carbon in and on the shank of the pulled capillary. Following pyrolysis, the capillary was left to cool for 20 s before its tip was rinsed with distilled water. To accomplish electrical connection, graphite powder was packed and a 10 A tin-coated copper fuse wire was introduced through the larger end of the capillary before it was sealed with epoxy.

Physically small carbon electrodes were then hydrogenated using a procedure reported by Bendavid et al.[25] In a radio frequency plasma-enhanced chemical vapor deposition setup, the electrodes were carefully placed with the pulled ends facing upward directly in the path of a stream of radio frequency plasma. Prior to hydrogenation, optimum conditions were achieved through establishing a base pressure of 1 mPa before hydrogen was fed at a flow rate of 25 mL min^{-1}. The process pressure was set at 6.6 Pa at a radio frequency (13.56 MHz) power of 200 W. Hydrogen gas was pumped into a vacuum chamber for 3 min to provide a hydrogen atmosphere around electrodes.

Electrochemical Characterization. To assess electrode functioning, cyclic voltammetry was conducted at bare and hydrogenated carbon electrodes using the following redox markers, 1.0 mM $Ru(NH_3)_6^{3+}$ in 1.0 M KCl as supporting electrolyte, 1.0 mM $Fe(CN)_6^{3-}$ in 1.0 M KCl as supporting electrolyte, and 1.0 mM dopamine in pH 7.4 citrate/phosphate buffer.

Surface Morphology Study. The morphology and chemical composition of hydrogenated carbon electrode surface were studied using several spectroscopic techniques. Atomic force microscopy was conducted using a homemade room-temperature confocal sample-scanning fluorescence microscope according to a published procedure.[26] Raman spectroscopy was performed on a Renishaw inVia microspectrometer fitted with a 1800 mm length grating and a 50× objective to focus the 514.5 nm line of an argon ion laser on the sample. X-ray photoelectron spectroscopy was carried out using an ESCALAB220i-XL (Thermo Scientific, United Kingdom).

dx.doi.org/10.1021/ac403283t | *Anal. Chem.* XXXX, XXX, XXX−XXX

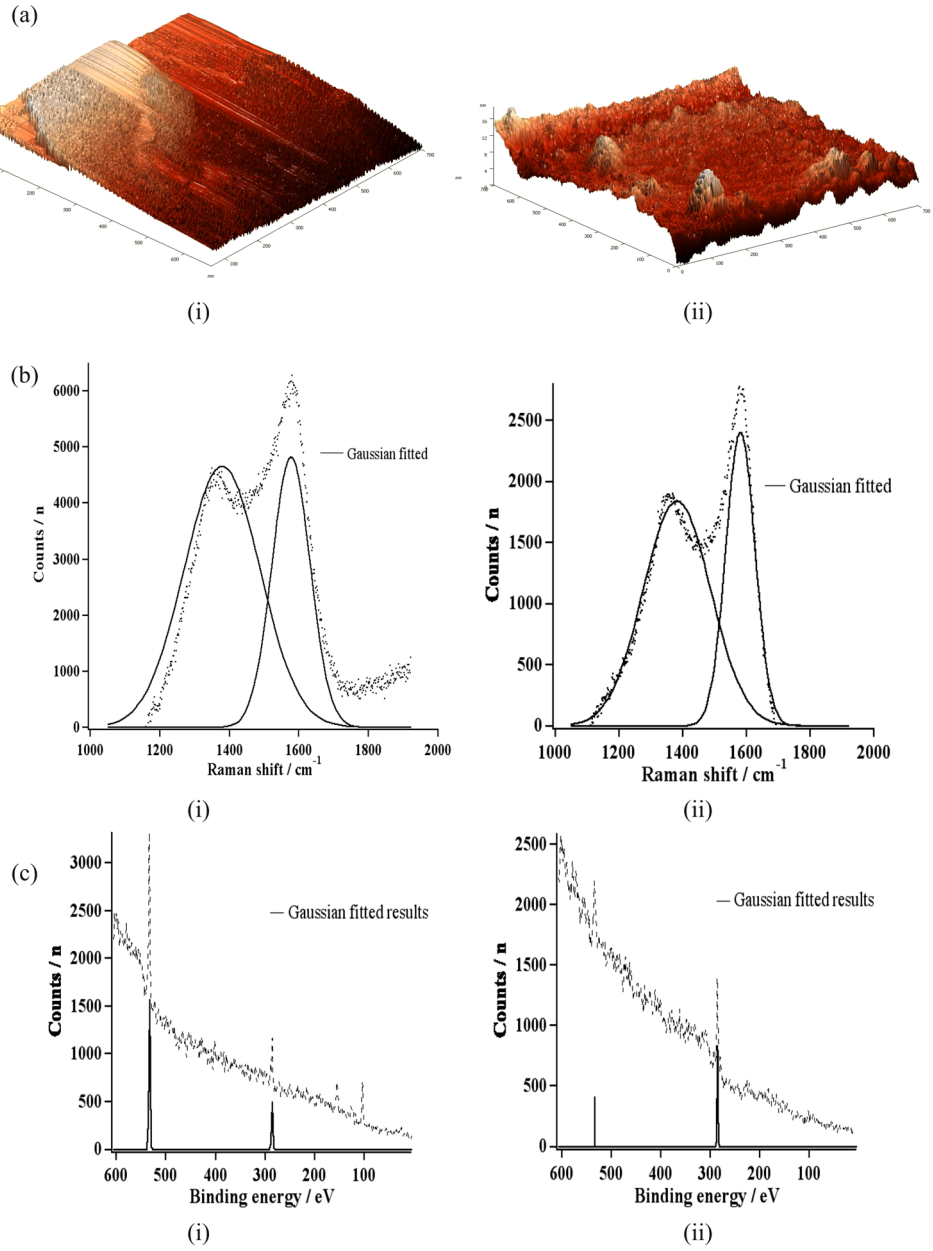

Figure 1. (a) Atomic force micrographs, (b) Raman spectra, and (c) X-ray photoelectron spectra of (i) a bare carbon electrode and (ii) a hydrogenated carbon electrode.

In Vivo Determination of Dopamine. All experiments were conducted by adhering to ethics approved by the Animal Ethics Committee at Macquarie University. A male Sprague–Dawley rat (303–330 g) was anesthetized with urethane (1.5 g kg^{-1} by intraperitoneal injection) before being mounted in a stereotaxic frame housed inside a Faraday cage to isolate noise. Next, a concentric bipolar stimulating electrode was implanted into the ventral tegmental area. A AglAgCl reference and stainless-steel auxiliary electrode combination was placed in surface contact with contralateral cortical tissue approximately 2.0 mm posterior to bregma. Either a bare or a hydrogenated conical-tip carbon working electrode was then implanted in the left striatum. Approximately 5 min following implantation of the recording electrode, a series of 0.5 ms duration cathodic monophasic current pulses (800 μA) was delivered to the stimulating electrode via an optical isolator and programmable pulse generator. Data acquisition was conducted using a potentiostat. A fixed potential of +0.9 V was applied and the dopamine released was monitored for 60 min. Current peaks, sampled at 10 000 bits s^{-1}, were compared at the start and end of the monitoring period to evaluate the degree of fouling. Where needed, Gaussian peak fitting was performed to distinguish overlapping signals. All signals were corrected for the 50 Hz mains cycle contribution. All results obtained in the in vivo experiments were evaluated based on four bare carbon electrodes and four hydrogenated carbon electrodes implanted in five rats.

Data Analysis. Wave slopes of all cyclic voltammograms were estimated from a plot of potential versus $\log_{10}[(I_{lim} - I)/I]$ (where I denotes current at a specific potential and I_{lim} the limiting current on the voltammogram), with the half-wave potential ($E_{1/2}$) being the intercept on the potential axis. The statistical significance of all correlation coefficients at the 95% confidence level was evaluated based on Student's t-test. Uncertainties associated with the slope and ordinate intercept

dx.doi.org/10.1021/ac403283t | Anal. Chem. XXXX, XXX, XXX–XXX

of all linear plots were expressed as confidence intervals at the 95% level.

RESULTS AND DISCUSSION

In this work, conical-tip carbon electrodes used for detection of dopamine were fabricated by pyrolyzing acetylene in and on the shank of a quartz capillary that was pulled down to a fine tip. As previously reported by us,[9] only electrodes that displayed a sigmoidal-shaped cyclic voltammogram in 1.0 mM $Ru(NH_3)_6^{3+}$ (in 1.0 M KCl supporting electrolyte) with a small charging current between the forward scan and the backward scan were used in further work. On the basis of analysis of chronoamperometric results,[12] the average radius of these electrodes was estimated to be 2 μm with a standard deviation of 0.5 μm and an average axial length of 4 μm with a standard deviation of 0.1 μm (N = 14). Next, these conical-tip carbon electrodes were subjected to hydrogenation. In this work, radio frequency plasma-enhanced chemical vapor deposition, instead of a remote microwave plasma-enhanced vapor deposition method,[9] was used to hydrogenate the carbon electrodes. The former technique is known to generate similar neutral and atomic hydrogen species to those encountered in microwave plasma-enhanced chemical vapor deposition, but without the accompanying high concentrations of active species such as excited hydrogen that are normally prevalent in a microwave-dependent plasma environment.[27] In this way, damage to the fine electrode tips was avoided during the hydrogenation step of the fabrication procedure.

Spectroscopic and Microscopic Examination of Electrode Surface. Initially, the surface morphology of carbon electrodes (N = 7) prior to and following hydrogenation was examined by atomic force microscopy, and the micrographs obtained are depicted in Figure 1a. At the bare carbon electrode, the surface appears to be nonhomogeneous with occurrences of islands of grainy texture at some locations along the electrode surface, which is in agreement with those reported by Rezek and Nebel.[28] On the basis of analysis of the heights of these carbon formations along the quartz surface, the roughness of the carbon deposit was estimated to be 0.5 μm. After hydrogenating the same electrode, the feature heights were estimated to be 8 nm, indicating a 1000-fold decrease in surface roughness. This is consistent with previous hydrogenation work in a plasma environment that yielded a reduction in the edge plane sites caused by atomic hydrogen present in the plasma, resulting in a smoother surface.[29]

Next, the hydrogenated electrode surface was studied by Raman spectroscopy and both the experimental and Gaussian-fitted results obtained are shown in Figure 1b. Here, two peaks, similar to those reported at a graphitized carbon surface, are observed at ~1230−1300 and 1579 cm^{-1}, respectively.[30] The first peak, referred to as an A_{1G} or "D" peak is attributable to disorder-induced Raman activity of the zone boundary or edge plane phonons at disordered clusters of sp^2 carbon sites,[31,32] while the second peak at 1579 cm^{-1} corresponds to an in-plane stretching mode, commonly termed as the E_{2G} or "G" peak[29,32] attributable to the bond stretching of all pairs of sp^2 atoms in both rings and chains.[31,32] A comparison of the respective intensities of the D and G peaks (D/G ratio) will thus indicate the sp^3 content of carbon films,[31] with the G peak Raman intensity strongly increasing with the H content.[33] In our work, a ratio of D/G peak heights of 0.97 (N = 7) and 0.77 (N = 7) was obtained at hydrogenated carbon and bare carbon electrodes, respectively. This increase in the ratio at hydrogenated carbon electrodes confirms a corresponding increase in hydrogen content following modification of the electrodes, in agreement with results reported by others, such as up to 0.75 for diamondlike carbon films.[34] Similarly, the Gaussian-fitted D and G peak area ratio was estimated to be 1.9 at bare carbon electrodes, which decreased to 1.7 at hydrogenated carbon electrodes.

Next, X-ray photoelectron spectroscopy was performed to characterize any organic materials on the electrode surface and to determine their molecular structure by probing the chemical states of the constituent elements.[35,36] Both the experimental and Gaussian-fitted results are presented in Figure 1c. There are two prominent bands at 284 and 532 eV that can be attributed to the presence of carbon, C_{1s},[29,37] and oxygen, O_{1s},[29,38,39] respectively. It is observed that there is a predominant O_{1s} peak in the spectrum for a bare carbon electrode, with an O_{1s}/C_{1s} peak height ratio of 2.0. Upon hydrogenation of the same electrode, however, there is considerable attenuation of the O_{1s}/C_{1s} peak ratio to 0.33 (N = 4). Notably, the reduction in oxygen content present on the electrode surface following hydrogenation is likely to be due to diminished oxygen-bearing functionalities (such as carbonyl, hydroxyl, and oxide groups) previously associated with sp^2 carbon on the electrode surface, which are eventually replaced by chemisorbed hydrogen atoms.[40]

Electrochemical Characterization of Hydrogenated Carbon Electrodes. In this work, we have initially characterized hydrogenated conical-tip carbon electrodes by comparing the cyclic voltammetric responses at these electrodes to those at bare conical-tip carbon electrodes in three redox systems: (i) 1.0 mM $Ru(NH_3)_6^{3+}$ in 1.0 M KCl, (ii) 1.0 mM $Fe(CN)_6^{3-}$ in 1.0 M KCl, and (iii) 1.0 mM dopamine in pH 7.4 citrate/phosphate buffer. The results of these experiments are presented in Figure 2.

As shown in Figure 2a, a sigmoidal-shaped cyclic voltammogram of 1.0 mM $Ru(NH_3)_6^{3+}$ in 1.0 M KCl supporting electrolyte was obtained. On bare carbon electrodes, reactive carbonyl and quinone-bearing sp^2-rich edge plane sites were present at the electrode surface.[41] Upon hydrogenation of such a surface, these functionalities were lost following the formation of C−H bonds. As an outer sphere, cationic redox analyte, the reaction of $Ru(NH_3)_6^{3+}$ is expected to be insensitive to the type of carbon surface before and after hydrogenation. However, we observed a 24% decrease (with standard deviation of 8%, N = 7) in the reduction current at the electrodes after hydrogenation. This is most likely caused by diminished conductivity at a hydrogen-terminated carbon surface. We also determined the wave slope and $E_{1/2}$ of the cyclic voltammograms, and the results are tabulated in Table 1. Following hydrogenation, $E_{1/2}$ slightly shifted to a more positive potential but the wave slope has deviated further from the expected 59.2 mV $decade^{-1}$, suggesting a less reversible reaction at the hydrogenated carbon electrodes.

Next, we characterized the electrodes by cyclic voltammetry of a second outer sphere, anionic redox analyte, $Fe(CN)_6^{3-}$, which is often used to evaluate the extent of surface activation[42] and to probe the effects of surface oxides via changes to reaction kinetics.[41,43] As shown in Figure 2b, there was a 39% increase (with a standard deviation of 4%, N = 7) in the reduction current of $Fe(CN)_6^{3-}$ obtained at hydrogenated carbon electrodes. This is consistent with an ~50% increase in the $Fe(CN)_6^{3-}$ reduction peak current observed at hydrogenated glassy carbon electrodes relative to bare glassy carbon electrodes.[42] The larger faradaic current at hydrogenated glassy carbon electrodes was attributed to their lower background current than that at bare glassy carbon electrodes.[42] As shown in Table 1, the wave slope for $Fe(CN)_6^{3-}$ reduction at hydrogenated carbon electrodes was similar to that

dx.doi.org/10.1021/ac403283t | Anal. Chem. XXXX, XXX, XXX−XXX

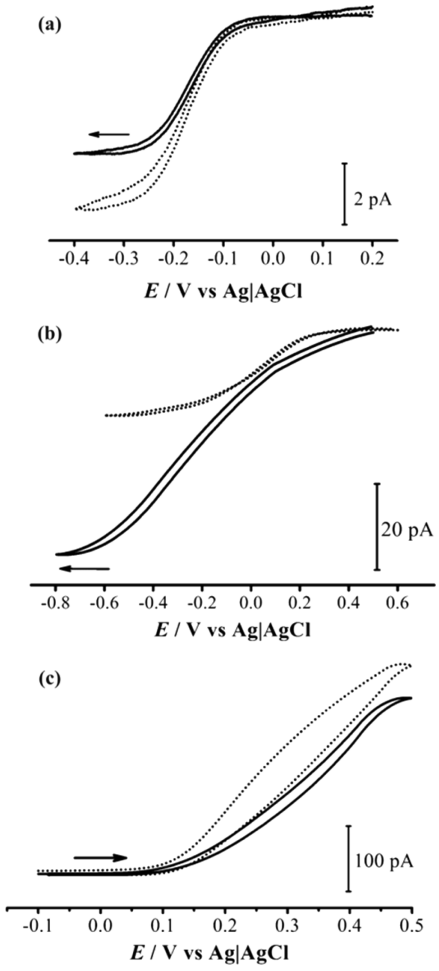

Figure 2. Cyclic voltammetry of (a) 1.0 mM $Ru(NH_3)_6^{3+}$ in 1.0 M KCl supporting electrolyte, (b) 1.0 mM $Fe(CN)_6^{3-}$ in 1.0 M KCl supporting electrolyte, and (c) 1.0 mM dopamine in pH 7.4 citrate/phosphate buffer at hydrogenated (solid line) and bare (dashed line) conical-tip carbon electrodes. Scan rate: 100 mV s^{-1} in all voltammograms. All arrows indicate the direction of the forward scan.

at bare carbon electrodes, suggesting minimal effect on the reversibility of the reduction. On the other hand, an unexpectedly large negative shift in the $E_{1/2}$ is observed at hydrogenated carbon electrodes, suggesting slower reaction kinetics at the modified surface. Further investigation is being conducted in our laboratory to examine the $Fe(CN)_6^{3-}$ reaction at structurally larger hydrogenated carbon electrodes.

Finally, the voltammetric signal for oxidation of dopamine is shown in Figure 2c. Notably, there is an 18% decrease (with a standard deviation of 3%, $N = 7$) in the oxidation current of the dopamine cyclic voltammogram at hydrogenated electrodes. This arises from fewer exposed edge planes at the hydrogenated carbon surface that catalyzes dopamine oxidation. The $E_{1/2}$ has also slightly shifted negatively, suggesting slower oxidation kinetics at the hydrogenated surface. This particular feature may aid in reducing the adsorption of the oxidation product, dopamine quinone, which would in turn cause electrode fouling.[44,45]

Analytical Performance of Hydrogenated Carbon Electrodes. On the basis of the steady-state chronoamperometric dopamine oxidation currents (a +0.9 V pulse applied at 0 V) at hydrogenated electrodes, we constructed the calibration plots shown in Figure 3a with the corresponding linear

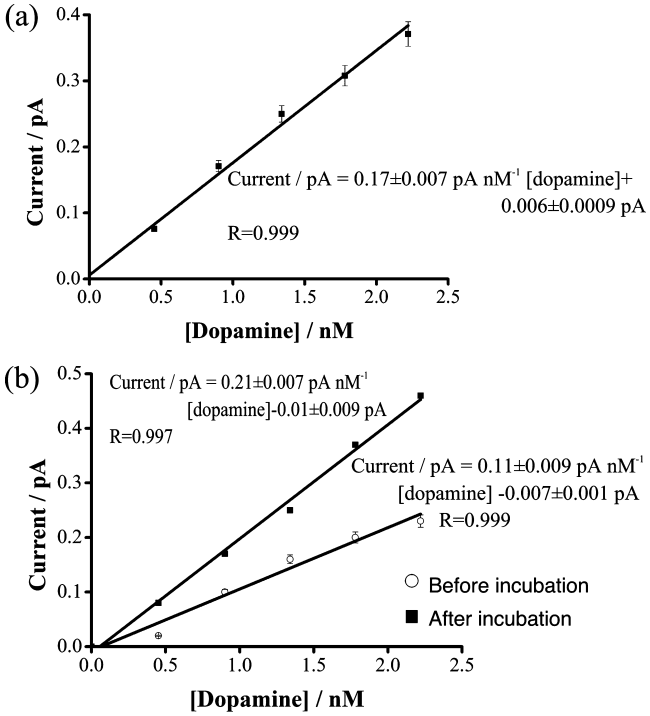

Figure 3. Calibration plots based on steady-state chronoamperometric dopamine oxidation currents (a) in pH 7.4 citrate/phosphate buffer at a hydrogenated electrode and (b) before and after incubation in 0.1% (w/v) bovine serum albumin + 1.0% (v/v) caproic acid + 0.002% (w/v) human fibrinopeptide B + 0.01% (w/v) cytochrome C in pH 7.4 citrate/phosphate buffer at hydrogenated conical-tip carbon electrodes.

expression and correlation coefficient obtained at these electrodes. The limit of detection (based on a signal-to-noise ratio of 3) and sensitivity (based on the slope of the linear calibration plot) were estimated to be 721 pM and 0.17 pA nM^{-1}, respectively.

Table 1. Wave Slope, $E_{1/2}$, and $|E_{3/4} - E_{1/4}|$ Estimated from Cyclic Voltammograms of the Redox Systems at Bare and Hydrogenated Conical-Tip Carbon Electrodes[a]

	redox system					
	$Ru(NH_3)_6^{3+}$		$Fe(CN)_6^{3-}$		dopamine	
electrochemical parameters	$E_{1/2}$ (mV)	wave slope (mV $decade^{-1}$)	$E_{1/2}$ (mV)	wave slope (mV $decade^{-1}$)	$E_{1/2}$ (mV)	wave slope (mV $decade^{-1}$)
bare carbon electrodes	−187 (7)	77 (3)	109 (35)	206 (25)	300 (16)	169 (5)
hydrogenated carbon electrodes	−177 (23)	110 (30)	−208 (9)	202 (30)	290 (3)	192 (23)

[a]All values in parentheses denote standard deviations estimated from seven repeated experiments. On the basis of a two-tailed Student's *t*-test, at the 95% confidence level, (i) there was no significant change in $E_{1/2}$ between bare and hydrogenated carbon electrodes and (ii) there were significant changes in wave slope only in the $Ru(NH_3)_6^{3+}$ and the dopamine reaction.

dx.doi.org/10.1021/ac403283t | Anal. Chem. XXXX, XXX, XXX−XXX

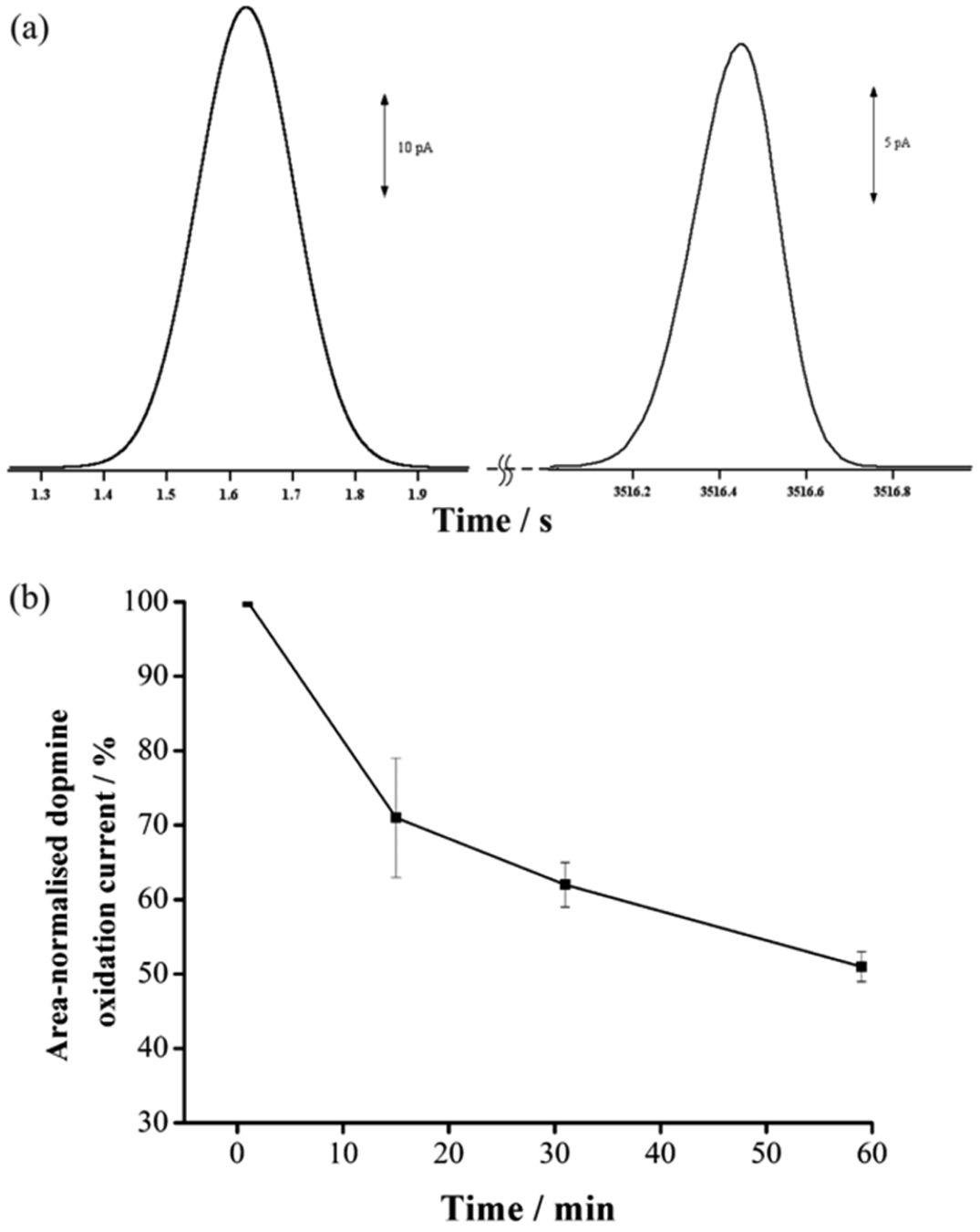

Figure 4. (a) Gaussian-fitted dopamine oxidation signals obtained upon repeated electrical stimulations in the rat striatum at the start and after 60 min of monitoring at a hydrogenated carbon electrode; (b) a plot of electrode area-normalized current measured at 60 min interval at hydrogenated carbon electrodes implanted in the rat striatum.

The limit of detection in our study compares favorably with 750 nM obtained at carbon electrodes hydrogenated by remote plasma hydrogenation.[9] Thus, the hydrogenated carbon electrodes in this study are expected to be able to detect low dopamine concentrations approaching 0.2−2.0 μM generally encountered in vivo.[46,47]

Electrode Performance in Solutions Containing Fouling Agents. Amphiphilic, high-molecular-weight proteins, peptides, and lipids present in biological matrixes can often adsorb on an electrode surface, prohibiting the analyte from making direct contact with the surface. Such fouling of the surface results in a diminishing transient electrode response. It is therefore useful to initially characterize the electrode performance before and after incubation in a fouling environment to discern the degree of electrode fouling. Accordingly, in this work, we have calibrated electrodes using chronoamperometry (a +0.9 V pulse applied at 0 V) of 1 mM dopamine in citrate/phosphate buffer before and after they were incubated for 7 days in a synthetic fouling solution consisting of 1.0% (v/v) caproic acid (a lipid), 0.1% (w/v) bovine serum albumin and 0.01% (w/v) cytochrome C (both are proteins), and 0.002% (w/v) human fibrinopeptide B (a peptide). The background current-subtracted results obtained are shown in Figure 3b. There was a ~45% increase in background current at carbon electrodes incubated in the synthetic fouling solution for 7 days, indicating a degree of fouling. However, dopamine was still oxidized at these electrodes

dx.doi.org/10.1021/ac403283t | *Anal. Chem.* XXXX, XXX, XXX−XXX

in the presence of the fouling agents, giving rise to currents plotted in Figure 3b. There was a 35% decrease in sensitivity at hydrogenated carbon electrodes following incubation in the fouling solution. Notably, very similar blank signals were obtained following incubation. Therefore, we have obtained a comparable limit of detection of 720−721 pM at electrodes before incubation.

In comparison, bare carbon electrodes subjected to the same fouling solution displayed significant changes in their response to dopamine. The data obtained consisted of widely scattered data points with a statistically nonsignificant correlation coefficient, impeding the estimation of limit of detection and sensitivity. We attribute this to extreme surface degradation that results at such bare carbon surfaces, in agreement with those previously reported.[48,49] On the basis of these findings, hydrogenated electrodes evidently displayed a degree of fouling-withstanding capabilities that is not achievable at bare carbon electrodes.

Dopamine Detection at Hydrogenated Electrodes in Vivo. To obtain a more realistic assessment of the effectiveness of hydrogenating bare carbon electrodes to withstand fouling, detection of dopamine in vivo was also performed. In these experiments, electrodes were implanted in the left striatum of a rat brain where dopamine vesicles occur in abundance, and the dopamine oxidation signal was monitored at the time of implanting and a defined period later. These signals, arising as a result of electrical stimulation of the ventral tegmental area, were monitored every 15 min for 60 min. For clarity, only Gaussian-fitted responses are shown. In Figure 4a, negligible current was generated in the absence of any stimulation between 0.0 s and approximately 0.25 s. Upon stimulations, dopamine release occurred at the synaptic cleft between two neurons. As dopamine reached the working electrode in the left striatum, it was immediately oxidized, giving rise to the oxidation peak between 0.25 and 0.35 s. The current decay resulted from depletion effects setting in through diffusion away from the synapse, interaction with receptors, and/or uptake by transporters.[8] Over time, as the adsorption of large molecular weight amphiphilic species gradually manifested on the electrode surface, a corresponding transient decrease in the dopamine oxidation signal resulted. On this premise, the extent of fouling of the electrode surface was estimated by the diminishing oxidation peak height.

Figure 4b shows a plot of the mean percentage of electrode area-normalized oxidation current remaining against time over which detection of dopamine was monitored at four hydrogenated carbon electrodes. Notably, the dopamine release was assumed to be quantitatively reproducible in all these experiments. At the commencement of the experiment, we assumed that negligible fouling occurred, and on this basis, the current remaining at the start was assigned 100%. At the hydrogenated carbon electrodes, 71% remaining dopamine oxidation current is observed at 30 min in a 60 min experiment, followed by a more gradual decline in signal thereafter to 50%. On the basis of slope measurements, the rate of fouling at hydrogenated carbon electrodes was estimated at 1.2% min^{-1} for the first 30 min, followed by a more gradual 0.7% min^{-1}. In contrast, bare carbon electrodes were previously shown to display an almost steady reduction trend in dopamine oxidation current, which corresponded to a fouling rate of 1.0% min^{-1}.[16] These results indicate that hydrogenated carbon electrodes appear to require an initial period to combat against adsorption of high-molecular-weight species before the fouling rate could be further retarded. To address this, the electrode tips may need to be subjected to the hydrogen stream in the plasma for a prolonged period to achieve more extensive hydrogenation. In this manner, the sp^2 carbon content can be further minimized, which would otherwise induce hydrophilic character on the electrode surface. Nonetheless, results presented in the current work do provide indication that hydrogenated carbon electrodes offer a degree of protection of carbon electrodes against fouling during dopamine detection in vivo.

■ CONCLUSIONS

In this work, we have studied the analytical characteristics of hydrogenated conical-tip carbon electrodes in dopamine detection in vivo. The hydrogenated carbon electrodes demonstrated negligible change in limit of detection and sensitivity after being incubated in a laboratory synthetic solution containing a number of fouling reagents. In comparison, bare carbon electrodes displayed unmeasurable limits of detection and sensitivity toward dopamine. In addition, during in vivo dopamine detection, at least 71% of the initial dopamine oxidation signal was still observable at hydrogenated carbon electrodes after the first 30 min of a 60 min continuous measurement and at least 50% observable during the remaining period of the experiment. These findings provide early evidence for hydrogenated conical-tip carbon electrodes in combating against fouling during in vivo detection experiments.

■ AUTHOR INFORMATION

Corresponding Author

*E-mail: Danny.Wong@mq.edu.au. Tel: +61-2-9850-8300.

Present Address

[‖]Shaneel Chandra: School of Biological and Chemical Sciences, Faculty of Science, Technology and Environment, The University of the South Pacific, Laucala Bay Campus, Suva, Fiji.

Notes

The authors declare no competing financial interest.

■ REFERENCES

(1) Budygin, E. A.; Park, J.; Bass, C. E.; Grinevich, V. P.; Bonin, K. D.; Wightman, R. M. *Neurosci.* **2012**, *201*, 331−337.

(2) Arya, S. K.; Singh, S. P.; Malhotra, B. D. In *Handbook of Biosensors and Biochips*; Marks, R. S., Cullen, D. C., Karube, I., Lowe, C. R., Weetall, H. H., Eds.; John Wiley & Sons, Ltd.: Chichester, 2007; Vol. *1*, pp 341−378.

(3) Park, J.; Takmakov, P.; Wightman, R. M. *J. Neurochem.* **2011**, *119* (5), 932−944.

(4) Bledsoe, J. M.; Kimble, C. J.; Covey, D. P.; Blaha, C. D.; Agnesi, F.; Mohseni, P.; Whitlock, S.; Johnson, D. M.; Horne, A.; Bennet, K. E.; Lee, K. H.; Garris, P. A. *J. Neurosurg.* **2009**, *111* (4), 712−723.

(5) Sombers, L. A.; Wittenberg, N. J.; Maxson, M. M.; Adams, K. L.; Ewing, A. G. *ChemPhysChem* **2007**, *8* (17), 2471−2477.

(6) Kim, D.; Koseoglu, S.; Manning, B. M.; Meyer, A. F.; Haynes, C. L. *Anal. Chem.* **2011**, *83* (19), 7242−7249.

(7) Miller, P. R.; Gittard, S. D.; Edwards, T. L.; Lopez, D. M.; Xiao, X.; Wheeler, D. R.; Monteiro-Riviere, N. A.; Brozik, S. M.; Polsky, R.; Narayan, R. J. *Biomicrofluidics* **2011**, *5* (1), 013415-14.

(8) Michael, D. J.; Wightman, R. M. *J. Pharm. Biomed. Anal.* **1999**, *19* (1−2), 33−46.

(9) Alwarappan, S.; Butcher, K. S. A.; Wong, D. K. Y. *Sens. Actuators, B* **2007**, *128* (1), 299−305.

(10) McNally, M.; Wong, D. K. Y. *Anal. Chem.* **2001**, *73* (20), 4793−4800.

(11) Wong, D. K. Y.; Blaha, C. D.; McNally, M. *Chem. Australia* **2003**, *70* (11), 12−15.

(12) Britz, D.; Chandra, S.; Strutwolf, J.; Wong, D. K. Y. *Electrochim. Acta* **2010**, *55* (3), 1272−1277.

(13) Park, J.; Quaiserova-Mocko, V.; Patel, B. A.; Novotny, M.; Liu, A.; Bian, X.; Galligan, J. J.; Swain, G. M. *Analyst* **2008**, *133* (1), 17−24.
(14) Finnerty, N. J.; O'Riordan, S. L.; Palsson, E.; Lowry, J. P. *J. Neurosci. Methods* **2012**, *209* (1), 13−21.
(15) Gerhardt, G. A.; Oke, A. F.; Nagy, G.; Moghaddam, B.; Adams, R. N. *Brain Res.* **1984**, *290* (2), 390−395.
(16) Chandra, S.; Miller, A. D.; Wong, D. K. Y. *Electrochim. Acta* **2013**, *101*, 225−231.
(17) Yoshimi, K.; Naya, Y.; Mitani, N.; Kato, T.; Inoue, M.; Natori, S.; Takahashi, T.; Weitemier, A.; Nishikawa, N.; McHugh, T.; Einaga, Y.; Kitazawa, S. *Neurosci. Res.* **2011**, *71* (1), 49−62.
(18) Garris, P. A.; Ensman, R.; Poehlman, J.; Alexander, A.; Langley, P. E.; Sandberg, S. G.; Greco, P. G.; Wightman, R. M.; Rebec, G. V. *J. Neurosci. Methods* **2004**, *140* (1−2), 103−115.
(19) Hafizi, S.; Kruk, Z. L.; Stamford, J. A. *J. Neurosci. Methods* **1990**, *33* (1), 41−49.
(20) Wang, S.; Swope, V. M.; Butler, J. E.; Feygelson, T.; Swain, G. M. *Diamond Relat. Mater.* **2009**, *18* (4), 669−677.
(21) Shang, F.; Zhou, L.; Mahmoud, K. A.; Hrapovic, S.; Liu, Y.; Moynihan, H. A.; Glennon, J. D.; Luong, J. H. T. *Anal. Chem.* **2009**, *81* (10), 4089−4098.
(22) Singh, Y. S.; Sawarynski, L. E.; Michael, H. M.; Ferrell, R. E.; Murphey-Corb, M. A.; Swain, G. M.; Patel, B. A.; Andrews, A. M. *ACS Chem. Neurosci.* **2009**, *1* (1), 49−64.
(23) Neitzel, I.; Mochalin, V.; Gogotsi, Y. In *Ultrananocrystalline Diamond*, 2nd ed.; William Andrew Publishing: Oxford, 2012; pp 421−456.
(24) Datta, J.; Ray, N. R.; Sen, P.; Biswas, H. S.; Vogler, E. A. *Mater. Lett.* **2012**, *71*, 131−133.
(25) Bendavid, A.; Martin, P. J.; Randeniya, L.; Amin, M. S. *Diamond Relat. Mater.* **2009**, *18* (1), 66−71.
(26) Bradac, C.; Gaebel, T.; Naidoo, N.; Rabeau, J. R.; Barnard, A. S. *Nano Lett.* **2009**, *9* (10), 3555−3564.
(27) Musil, J. *Vacuum* **1986**, *36* (1−3), 161−169.
(28) Rezek, B.; Nebel, C. E. *Diamond Relat. Mater.* **2006**, *15* (9), 1374−1377.
(29) Chen, Q.; Swain, G. M. *Langmuir* **1998**, *14* (24), 7017−7026.
(30) Armandi, M.; Bonelli, B.; Geobaldo, F.; Onida, B.; Ferroni, M.; Otero Areán, C.; Garrone, E. In *Studies in Surface Science and Catalysis*; Čejka, J., Ĭílková, N., Nachtigall, P., Eds.; Elsevier: Amsterdam, 2005; Vol. *158*, Part A, pp 509−516.
(31) Filik, J.; May, P. W.; Pearce, S. R. J.; Wild, R. K.; Hallam, K. R. *Diamond Relat. Mater.* **2003**, *12* (3−7), 974−978.
(32) Goswami, R.; Jana, T.; Ray, S. *J. Phys. D: Appl. Phys.* **2008**, *41* (15), 155413.
(33) Casiraghi, C. *Diamond Relat. Mater.* **2011**, *20* (2), 120−122.
(34) Choi, J.; Ishii, K.; Kato, T.; Kawaguchi, M.; Lee, W. *Diamond Relat. Mater.* **2011**, *20* (5−6), 845−848.
(35) Swift, A. J. *Microchim. Acta* **1995**, *120* (1), 149−158.
(36) Sabbatini, L.; Zambonin, P. G. *J. Electron Spectrosc. Relat. Phenom.* **1996**, *81* (3), 285−301.
(37) Selvaraju, T.; Ramaraj, R. *J. Electroanal. Chem.* **2005**, *585* (2), 290−300.
(38) Xiao, Y.; Guo, C.; Li, C. M.; Li, Y.; Zhang, J.; Xue, R.; Zhang, S. *Anal. Biochem.* **2007**, *371* (2), 229−237.
(39) Yan, X. B.; Xu, T.; Yang, S. R.; Liu, H. W.; Xue, Q. J. *J. Phys. D: Appl. Phys.* **2004**, *37* (17), 2416−2424.
(40) Xu, J.; Chen, Q.; Swain, G. M. *Anal. Chem.* **1998**, *70* (15), 3146−3154.
(41) Ji, X.; Banks, C. E.; Crossley, A.; Compton, R. G. *ChemPhysChem* **2006**, *7* (6), 1337−1344.
(42) Fagan, D. T.; Hu, I. F.; Kuwana, T. *Anal. Chem.* **1985**, *57* (14), 2759−2763.
(43) Holloway, A.; Wildgoose, G.; Compton, R.; Shao, L.; Green, M. *J. Solid State Electrochem.* **2008**, *12* (10), 1337−1348.
(44) Safavi, A.; Maleki, N.; Moradlou, O.; Tajabadi, F. *Anal. Biochem.* **2006**, *359*, 224−229.
(45) Wang, H.-S.; Li, T.-H.; Jia, W.-L.; Xu, H.-Y. *Biosens. Bioelectron.* **2006**, *22* (5), 664−669.
(46) Lane, R. F.; Blaha, C. D.; Hari, S. P. *Brain Res. Bull.* **1987**, *19* (1), 19−27.
(47) Schenk, J. O.; Miller, E.; Rice, M. E.; Adams, R. N. *Brain Res.* **1983**, *277* (1), 1−8.
(48) Fujishima, A.; Rao, T. N.; Popa, E.; Sarada, B. V.; Yagi, I.; Tryk, D. A. *J. Electroanal. Chem.* **1999**, *473*, 179−185.
(49) Hashemi, P.; Dankoski, E. C.; Petrovic, J.; Keithley, R. B.; Wightman, R. M. *Anal. Chem.* **2009**, *81* (22), 9462−9471.